Crossing the frontier of validity of the material time approach in the aging of a molecular glass

Marceau Hénot, Xuan An Nguyen, François Ladieu

Crossing the Frontier of Validity of the Material Time Approach in the Aging of a Molecular Glass

Marceau Hénot,[1] Xuan An Nguyen,[1] and François Ladieu[1]

[1] *SPEC, CEA, CNRS, Université Paris-Saclay, CEA Saclay Bat 772, 91191 Gif-sur-Yvette Cedex, France.*[*]

We studied the physical aging of glycerol in response to upward temperature steps of amplitude ranging from 0.3 to 18 K. This was done using a specially designed experimental setup allowing to quickly heat up a liquid film while measuring the evolution of its dielectric properties. Despite the non-linear evolution of these observables for large steps, a fictive temperature could be obtained. In the case of moderate step amplitudes, we checked that the material time approach in its simplest form, the Single Parameter Aging (SPA) applies well. The memory kernel extracted from the quasi-linear regime was used to test its frontiers of validity for significant step amplitudes. We showed that the observations deviate from the prediction of the material time framework and of the SPA simultaneously. As these approaches link aging to equilibrium dynamics, our results help setting the bounds beyond which new theoretical arguments are needed.

Glasses are systems whose disordered structure resembles that of liquids, but that appear stuck in an out-of-equilibrium state due to prohibitively long relaxation times. They are nevertheless evolving towards their state of equilibrium through microscopic relaxation [1]. The resulting evolution of their macroscopic properties is called physical aging and is of practical importance for a wide range of materials. Its effect during the production of network glasses controls their final properties [2] whereas for final products, it can be responsible for unwanted drift of physical properties such as electrical resistivity [3], gas permeability of polymer films [4], or stability of amorphous pharmaceutical products [5]. From a fundamental perspective, the study of aging provides information on the out-of-equilibrium relaxation mechanisms [6, 7].

A typical aging experiment consists in setting a system out-of-equilibrium, for instance by the application of a mechanical load [8], a static electric field [9] or a change in temperature [10–18], and observing its reequilibration dynamics through the evolution of a quantity such as its enthalpy [16, 18], density [19], refractive index [18] or dielectric quantities [12–15]. In an ideal step experiment, care is taken to destabilize the system quickly enough so that no relaxation occurs, thus simplifying the interpretation of aging dynamics [9, 14, 15, 20, 21]. When the amplitude of the perturbation is extremely small, the response is linear (*i.e.* simply proportional to the perturbation amplitude) [15]. However, temperature step experiments are usually not in this regime, as an amplitude of only a few kelvins already yields a non-linear response. This is related to the extreme dependence of the equilibrium relaxation time with temperature that easily leads to a significant contrast in the dynamics of the initial and final states. This is called the fictive temperature effect and leads to an asymmetry of approach: reaching equilibrium is faster when starting from an initially higher temperature than from a smaller one. The Tool-Narayanaswamy (TN) formalism [2, 22] was shown to be very powerful at quantitatively describing this effect [9, 14, 15, 17–20, 23–26]. It is based on the idea of a *material time* with respect to which the system responds linearly and homogeneously to even significantly large perturbations. This material time flows at a rate controlled by an out-of-equilibrium relaxation time that itself ages. The performance of this phenomenological model has motivated recent studies aiming at investigating the potential deeper physical meaning of the material time [16, 27–29]. When the temperature step amplitude, and thus the distance from equilibrium, is increased, deviations from the TN prediction start to be perceptible [15, 18]. An extreme illustration is the heterogeneous equilibration dynamics observed in ultrastable glasses [30] which display an exceptional stability [31, 32]. Their annealing close to the glass transition temperature T_g can be compared to an extremely large temperature step experiment. In strong contrast with the homogeneous picture of the TN formalism, their aging dynamic was shown to be controlled by the nucleation and growth of equilibrated regions [33–35].

In this article, we study the aging of supercooled glycerol in response to upward temperature steps and we focus on characterizing how the material time approach starts to fail when increasing the step amplitude. Large ideal upward temperature steps are notoriously difficult to achieve experimentally as they either require a long equilibration phase below T_g or a high temperature change rate. We developed an original experimental setup allowing to quickly heat up a 25 μm thick glycerol film and maintain it at a constant temperature while

[*] marceau.henot@cea.fr

measuring the evolution of its dielectric properties. The 40 ms long heating phase, 50 times faster than state of the art setup [14, 15] and 2000 times faster than commercial setups, allows to apply large ideal temperature steps from an equilibrium state. Starting from small step amplitudes close to the linear regime, we check the validity of the material time approach in the moderate amplitude regime. By extracting in this framework the out-of-equilibrium relaxation time, we analyze how it progressively fails when increasing the step amplitude well below the limit at which the heterogeneous process takes over.

The experimental setup (see fig. 1a and SI) allows to apply to a liquid, initially equilibrated at T_0, a change in temperature within a time $t_\mathrm{h} = 40$ ms with an amplitude ΔT ranging from +0.3 to +18 K. The temperature is then maintained constant at $T_1 = T_0 + \Delta T$ during up to $t_\mathrm{max} = 50$ s by injecting on one side of the film a controlled heat flux through a sequence of heat pulses (see inset of fig. 1b) [21]. This technique, is by nature, limited to upward temperature steps. The response of the liquid is probed through the complex capacitance $C^\star = C' - jC''$ measured at fixed frequency f of an Interdigitated Electrodes system (IDE) in contact with the other side of the film. This quantity is directly related to the dielectric permittivity $\epsilon^\star$ of the liquid in the first few micrometers near the electrodes [36, 37]. The temperature step itself can be characterized at a high enough temperature T_0 so that the relaxation time $\tau_\alpha(T_0 = 207\ \mathrm{K}) \approx 8$ ms is shorter than t_h and the capacitance measurement can be used as a thermometer. The temperature, denoted $T_{\mathrm{from}\ C}(t)$, is obtained by mapping the capacitance measured at equilibrium (see SI). The result is shown in fig. 1b and it can be checked that beyond the 5% total amplitude sawtooth oscillations resulting from the heating pulses (see fig. 1b), the temperature stays constant within a range smaller than 2% of ΔT. These small variations are reproducible and are taken into account in the data analysis.

At low initial temperature T_0, the relaxation time of the liquid is much longer than t_h and a temperature step sets the liquid out-of-equilibrium in an ideal manner *i.e.* without letting the system relax during the heating (see SI). Fig. 1c displays the measurement of $C'(t)$ and $C''(t)$ at $f = 1.12$ kHz (top) and $f = 3.0$ kHz (bottom) following a step of amplitude $\Delta T = 10.2$ K starting from $T_0 = 188$ K. For all data, we observe a fast change during the heating phase, followed by a slow evolution (here during ≈ 5 s) before a plateau is reached. As shown in fig. 1d, these data can be converted in temperature units $T_{\mathrm{from}\ C}$ by mapping them with the equilibrium capacitance values. Except for $t < 0$ and after equilibration, this quantity does not correspond to the temperature of the phonons as the system is out-of-equilibrium. It is interesting to note that, although the four curves ($C'(t)$ and $C''(t)$ at both frequencies) do not follow exactly the same dynamics (this is especially visible for $f = 1.12$ kHz), all those data collapse well once plotted into temperature units. The inset of fig. 1d, which is a short time zoom, shows that $T_{\mathrm{from}\ C}$ partially follows the temperature change. This corresponds to the glassy response of the system that can be associated with the volume change and the effect of fast processes [38]. The slower evolution that follows corresponds to physical aging. The quantity, well suited by construction, to describe this out-of-equilibrium response in temperature units, is the fictive temperature T_f [39], made continuous by the subtraction of the glassy response. A traditional way to obtain it is to assume that the glassy response varies linearly with T with a constant slope measured below T_g. However, in this frequency range, and for large ΔT, the dielectric response of such a polar liquid does not evolve linearly with the temperature in the liquid regime. To overcome this problem, we chose to obtain $T_\mathrm{f}(t)$ by applying the classical procedure to $T_{\mathrm{from}\ C}$ rather than to C' or C''. This corresponds to assume that:

$$\Delta T_{\mathrm{from}\ C}(t) = \kappa \Delta T + (1-\kappa)\Delta T_\mathrm{f}(t) \qquad (1)$$

where κ is a coefficient characterizing the glassy response, *i.e.* the fraction of the $\Delta T_{\mathrm{from}\ C}$ step occurring during the heating phase. It is determined on each dataset by ensuring continuity of T_f ($\Delta T_\mathrm{f}(t=0) = 0$). Increasing the step amplitude from 0.3 to 18 K leads to a 20 % decrease in κ which could be due to the effect of β relaxation occurring during the heating phase [15]. For the smallest step amplitude, the values of κ are almost the same for C' and C'', but they differ for larger steps (see SI). This can be due to the fact that C', contrary to C'', is sensible to the high-frequency polarizability of the liquid ϵ_∞ that can have a different glassy response [9]. This is a limitation of the method by which we obtain T_f that starts to have consequences for the largest steps performed in this work ($\Delta T \geq 15$ K). But as detailed below, for those large steps the physical relevance of T_f itself is in question. The resulting fictive temperature evolution, locally averaged over a log time scale to remove the saw-tooth oscillations, is shown in fig. 1e. The protocol is validated by the fact that, for already such a large ΔT, C' and C'' measured at two different frequencies, despite displaying slightly different evolution, all lead to the same T_f up to significantly large step amplitudes.

The response of glycerol to temperature steps of amplitude ranging from 0.34 K to 17.9 K was measured with initial temperature between $T_0 = 193$ K and 184 K chosen to maximize the ideality of the step experiment (*i.e.* to keep the initial relaxation time large compared to t_h, its decrease with ΔT can to be compensated by decreasing T_0, see more details in SI). The resulting normalized fictive temperature evolution $\Delta T_\mathrm{f}/\Delta T$ (obtained from the average between C' and C'') is shown in fig. 2a. For the smallest step amplitude, the *transformation time*, *i.e.* the time needed for complete reequilibration of the liquid, is of the order of a few $\tau_\alpha(T_1)$. As the step amplitude increases, the transformation time also increases with respect to the equilibrium relaxation time, reaching $40\tau_\alpha(T_1)$ for $\Delta T = 17.9$ K. This is a consequence of the fictive temperature effect: the out-of-equilibrium relaxation time of the system is initially much larger than

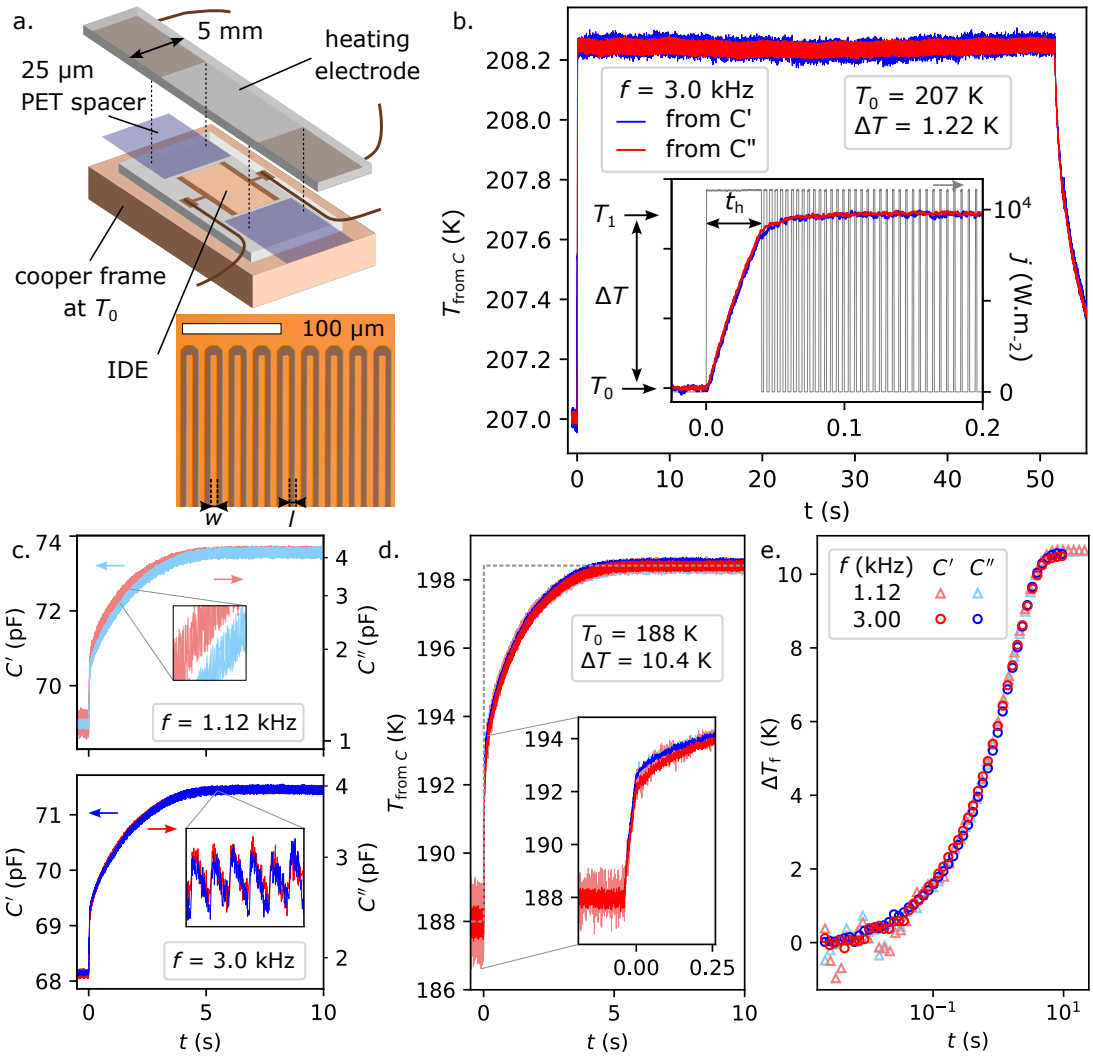

FIG. 1. (a) Schematic of the experimental setup consisting of a heating Indium-Tin-Oxyde electrode and an IDE separated by a 25 µm thick spacer and sandwiching a (not shown) glycerol film. A magnified picture of the IDE is shown. (b) Characterization of the temperature step measured at $T_0 = 207$ K using C' (blue) and C'' (red) as a thermometer. The inset shows a zoom on the heating phase of duration t_h and on the applied heating flux sequence (grey) used to heat and then maintain a constant temperature. (c-e) Response of the liquid to a temperature step of amplitude $\Delta T = 10.2$ K starting from $T_0 = 188$ K (c) Raw measurements of C' (blue) and C'' (red) at $f = 1.12$ kHz (top) and $f = 3.0$ kHz (bottom). The inset is a zoom showing saw-tooth oscillations originating from the heating flux sequence. (d) Same as c. plotted in temperature units. The actual temperature is shown with a dashed grey line. The inset is a short-time zoom. (e) Fictive temperature evolution ΔT_f obtained from eq. 1.

$\tau_\alpha(T_1)$. As for the magnitude of this effect, it can be compared to the $200\tau_\alpha(T_1)$ measured on the same liquid for $\Delta T = 45$ K [21] and the $10^6\tau_\alpha(T_1)$ for the rejuvenation of an ultrastable glass (with $\Delta T \approx 60$ K) [33].

In the TN framework, the material time ξ is controlled by the out-of-equilibrium relaxation time of the system $\mathrm{d}t = \tau(T, T_f)\mathrm{d}\xi$. Upon aging, this makes ξ flow at a variable rate compared to the observer time t. The central assumption is that with respect to the material time, the system responds linearly to any perturbation $T(\xi)$:

$$T_f(\xi) = T(\xi) - \int_0^\xi M(\xi - \xi')\frac{\mathrm{d}T}{\mathrm{d}\xi'}\mathrm{d}\xi' \qquad (2)$$

where M is the memory kernel of the system. For an ideal temperature step, $T(\xi > 0) = T_0 + \Delta T$, $\frac{\mathrm{d}T}{\mathrm{d}\xi'} = \Delta T\delta(\xi')$ where δ is a Dirac delta function. The evolution of fictive temperature is thus directly linked to M:

$$\Delta T_f(\xi) = \Delta T(1 - M(\xi)) \qquad (3)$$

It was shown that, for organic liquid, the material time governing aging is the same than the one controlling the α peak measured by dielectric spectroscopy [14] and that for moderate temperature steps the out-of-equilibrium relaxation time has no memory, meaning that $\tau(t) = \tau(T(t), T_f(t))$ [20]. This implies that all relaxation modes constituting the spatially heterogeneous dynamics, age

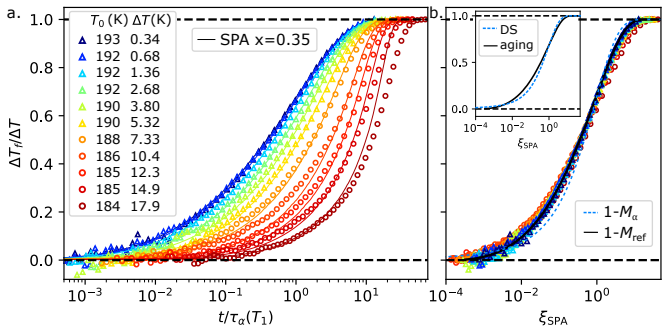

FIG. 2. (a) Normalized response $\Delta T_f/\Delta T$ as a function of $t/\tau_\alpha(T_1)$ to temperature steps of amplitude ranging from 0.34 K to 17.9 K and with decreasing T_0 to maximize step ideality. Solid lines correspond to the SPA prediction with $x = 0.35$. (b) Same quantity plotted as a function of the material time ξ_{SPA} computed from the SPA with $x = 0.35$. The black solid line corresponds to the reference kernel obtained from the smoothed mixed data of $\Delta T < 0.68$ K. The blue dashed line is a memory kernel obtained from equilibrium dielectric spectra. The inset shows only these two.

at the same homogeneous rate, controlled by τ, and obey a time aging-time superposition [40]. This justifies the characterization of the out-of-equilibrium state by a unique scalar quantity T_f.

The main challenge in applying the TN formalism is the knowledge of the out-of-equilibrium relaxation time $\tau(T, T_f)$. In the case of an Arrhenian dependence of τ_α, one simple way to express it is [2, 41]:

$$\ln \tau(T, T_f) = x \ln \tau_\alpha(T) + (1 - x) \ln \tau_\alpha(T_f) \qquad (4)$$

where x is the non-linearity parameter which is system dependent. It expresses the relative importance of the effects of the temperature bath T and of the out-of-equilibrium structure characterized by T_f. The case of liquids displaying a super-activated behavior is, in principle, more complex, but for small enough temperature step amplitude, the single parameter aging formalism (SPA) leads to an excellent agreement with experiments [15, 24, 25]. In this approach, $\ln \tau(t)$ is assumed to be given by:

$$\ln \tau(t) = \ln \tau_\alpha + \Lambda(X(t) - X_{eq}) \qquad (5)$$

where $X(t)$ is a measured physical quantity (that plays the role of T_f) and Λ is related to x. This is equivalent to a Taylor expansion of eq. 4 which can be rewritten as:

$$\ln \tau(T, T_f) = \ln \tau_\alpha(T) + (1 - x) \left. \frac{d \ln \tau_\alpha}{dT} \right|_T (T_f - T) \qquad (6)$$

By definition, the memory kernel M is the response to an extremely small temperature step. With a precise enough experimental setup, it can be measured directly as in ref. [15] for relative amplitude $\Delta T/T_1$ smaller than 0.06 %, and then used to independently test the SPA and demonstrate the existence of a material time. Another way, that does not require a direct measurement of M, is to consider the non-linear responses of two steps of different amplitudes and to transform one data-set into another using the SPA [25] (eq. 6). In the present work, we use an intermediate approach by considering the response to small step amplitudes $\Delta T < 0.7$ K that are not strictly in the linear regime. For these, the relaxation time is nevertheless dominated by the first term of eq. 6 and ξ_{SPA} is thus only weakly dependent on the value of x. On the one hand, this does not allow to precisely determine x and we can only state that it lies in the range $x \in [0.1; 0.6]$ (see SI). On the other hand, this provides a way to determine the kernel without making a strong assumption on x or even on the form of $\tau(T, T_f)$. We obtained $M(\xi)$ by merging and smoothing the data coming from the two datasets $\Delta T = 0.34$ and 0.68 K with $x = 0.35$ chosen as the middle of the range. The result $M_{ref}(\xi)$ is shown in fig. 2b as a solid line. This kernel characterizes the time distribution controlling the structural recovery of the system. It is far from exponential with a stretching coefficient of $\beta = 0.50$, almost identical to the 0.51 determined in ref. [17] on glycerol using shear rheology as a probe of aging. As the kernel corresponds to the linear response of the system to a change in temperature, it is interesting to compare it to the linear response to another kind of perturbation. The blue dashed line in fig. 2b corresponds to a kernel M_α obtained from dielectric spectra (see SI) which is the response to a small change in electric field. Although the mean time scale is very close, M_α appears slightly more exponential than M_{ref} ($\beta = 0.65$). For the reasons mentioned above related to the paradoxical homogeneous structural recovery while the structural relaxation is known to be spatially heterogeneous, the question of how these two time-scale distributions compare to each other is an actual question in the literature [9, 40, 42].

The reference kernel M_{ref} can be used to compute the prediction of the SPA. The non-linearity parameter giving the best agreement at moderate step amplitude ($\Delta T < 4$ K) is $x = 0.35$ with the result shown with solid lines in fig. 2a. This value is not very far from the $x = 0.29$ obtained in ref. [17] on glycerol. As expected, the agreement with experiments is very good in this range of moderate ΔT but progressively worsens as ΔT increases (see SI). It qualitatively captures the increase of the transformation time with ΔT but underestimates it by a factor of 2 for $\Delta T = 17.9$ K. Another way to assess the validity of the SPA is to plot the normalized response as a function of ξ_{SPA} as in fig. 2b: it is the kernel that would reproduce the experimental results with the SPA. While the data collapses well on the reference kernel for moderate step amplitude, this is not the case for larger steps. As shown in the SI, with the SPA, no value of x gives a satisfactory agreement for large temperature steps. This is not a surprise as it is expected by construction that the SPA should fail when $T_f - T$ is too large. The quantitative limit that we find (≈ 4 K or ≈ 2 % of relative temperature change) is of the same order as

what was reported for glycerol [25] or other systems in the case of upward steps [15, 18].

The value of the non-linearity parameter x extracted above deserves to be commented as it gives quantitative information on the role of T and T_f for this particular system. Ideal temperature steps are assumed to be isostructural transformations: contrary to the temperature bath, the structure of the liquid has not had the time to change. Under the assumption that the out-of-equilibrium states can be mapped onto equilibrium states [20], some authors have taken advantage of the density scaling approach [16, 43]. Indeed, the equilibrium relaxation time of liquids can usually be described by only one parameter Γ that itself depends on T and on the specific volume [44, 45]. Recently Di Lisio *et al.* [16] assumed that the mapping between τ and its equilibrium values could be obtained by considering Γ at the temperature of the phonons and at the out-of-equilibrium density, thus allowing to compute τ without any free parameter. However, in the specific case of glycerol and in the limit of small step amplitude, this approach gives $x \approx 0.85$ ([45, 46] see SI), out of the range of acceptable values mentioned above. This discrepancy may be related to the low density scaling exponent of glycerol compared to the five liquids studied by the authors. Nevertheless, it is important to note that the aforementioned approach is not the only one proposed in the literature. Niss [43] made a different conjecture that carefully separates the effect of the kinetic temperature bath (controlled by Γ computed as above) and of the scaled activation energy (described by a "fictive" Γ). Although our experiments do not allow to check quantitatively this conjecture, we note that, in comparison with the approach mentioned above, it predicts a smaller x value by reducing the influence of the temperature bath in τ, and thus bringing its value closer to our measurements (see SI).

As the SPA is a version of the TN in which $\tau(T, T_\mathrm{f})$ has a particularly simple form, one might ask whether there is a range of step amplitude for which a more complex form of $\tau(T, T_\mathrm{f})$ would give a better agreement. For example, the next order of the Taylor expansion may be required to describe larger distances from equilibrium. There are also a lot of different analytical forms for τ proposed in the literature [19, 47]. In order to answer this question, we take advantage of the reference kernel determined above to extract $\tau(T, T_\mathrm{f})$ from the experimental data by relying on a TN central assumption: $M(\xi)$ is independent of ΔT. As shown in fig. 3a, the measured normalized response is mapped onto the reference kernel to link the observer and material times using the relation:

$$\frac{\Delta T_\mathrm{f}(t)}{\Delta T} = 1 - M_\mathrm{ref}(\xi) \tag{7}$$

The result $t(\xi)$ is plotted with markers in fig. 3b for various step amplitudes. For the smallest one (in blue), the relationship is almost linear. This is expected as in the case of an infinitely small step: $t = \tau_\alpha(T_1)\xi$. For the largest step (in red) the concave shape connects the initial slow dynamics to the final faster one. The out-of-equilibrium relaxation time is given by:

$$\tau(T, T_\mathrm{f}) = \left.\frac{\mathrm{d}t}{\mathrm{d}\xi}\right|_{T,T_\mathrm{f}} \tag{8}$$

The result of the differentiation of the experimental data is shown in fig. 3c alongside with the equilibrium relaxation time $\tau_\alpha(T)$ (in grey). This procedure, although not identical, is equivalent to the one used in ref. [20]. All datasets follow the same behavior: the upward temperature jump corresponds to a downward jump in relaxation time from $\tau_\alpha(T_0)$ to $\tau_0 = \tau(T_1, T_\mathrm{f} = T_0)$. A progressive decrease follows until the final value $\tau_1 = \tau(T_1, T_\mathrm{f} = T_1)$ is reached. As a reference, the SPA with $x = 0.35$ is shown as solid black lines. A way to compare all datasets with respect to each other, shown in fig. 3d, is to plot the ratio $\tau/\tau_\alpha(T_1)$ as a function of the distance from equilibrium $(T_\mathrm{f} - T_1)|d \ln \tau_\alpha / dT|_{T_1}$. Following eq. 6, with the SPA, all data should collapse on a single straight line of slope $1 - x$. As expected from the above discussion, it is the case only for the moderate steps ($\Delta T < 4$ K). Surprisingly, in all cases, the initial relaxation time τ_0 is close to the one predicted by the SPA and the discrepancy comes from the final time τ_1. For the smaller steps, it meets well the equilibrium relaxation time $\tau_\alpha(T_1)$ (shown as black crosses). However, as ΔT increases, a discontinuity between these two values appears and grows. The ratio $\tau_1/\tau_\alpha(T_1)$ is plotted in fig. 3e. For $\Delta T < 0.7$ K it is equal to 1 by construction as those data are used to determine M_ref. It then displays a small but visible increase even for moderate step amplitude and excess 2 for the largest steps. This is much larger than the uncertainty on τ_1 resulting from the $\pm 1\%$ uncertainty on ΔT. It is important to recall that τ is not measured here, it is deduced assuming that the TN holds. This discontinuity of the relaxation time which seems physically impossible should be seen as a consequence that the TN does not apply. Imposing $\tau_1 = \tau_\alpha(T_1)$ would require making M dependent on ΔT and would be incompatible with the linear response assumption of the TN. Consequently, in the case of upward temperature steps of more than a few percent of relative amplitude, the memoryless assumption of $\tau(t)$ becomes less and less valid. This means that changing the form $\tau(T, T_\mathrm{f})$ beyond the SPA would not lead to a better agreement and the frontier of validity of the material time approach is very close to the one of the SPA. It should be noted that the deviation from the TN that we discuss here is visible but weak. By letting some freedom in the kernel (which would not make sense in the framework of this study), it would be possible to get a better agreement. This is consistent with the fact that in ref. [21], despite the larger distance to equilibrium, the TN approach helped in getting a qualitative understanding of the aging behavior following a complex thermal treatment.

The aging of very far-from-equilibrium systems has been reported to be very different from the homogeneous picture of TN approach. The reequilibration of

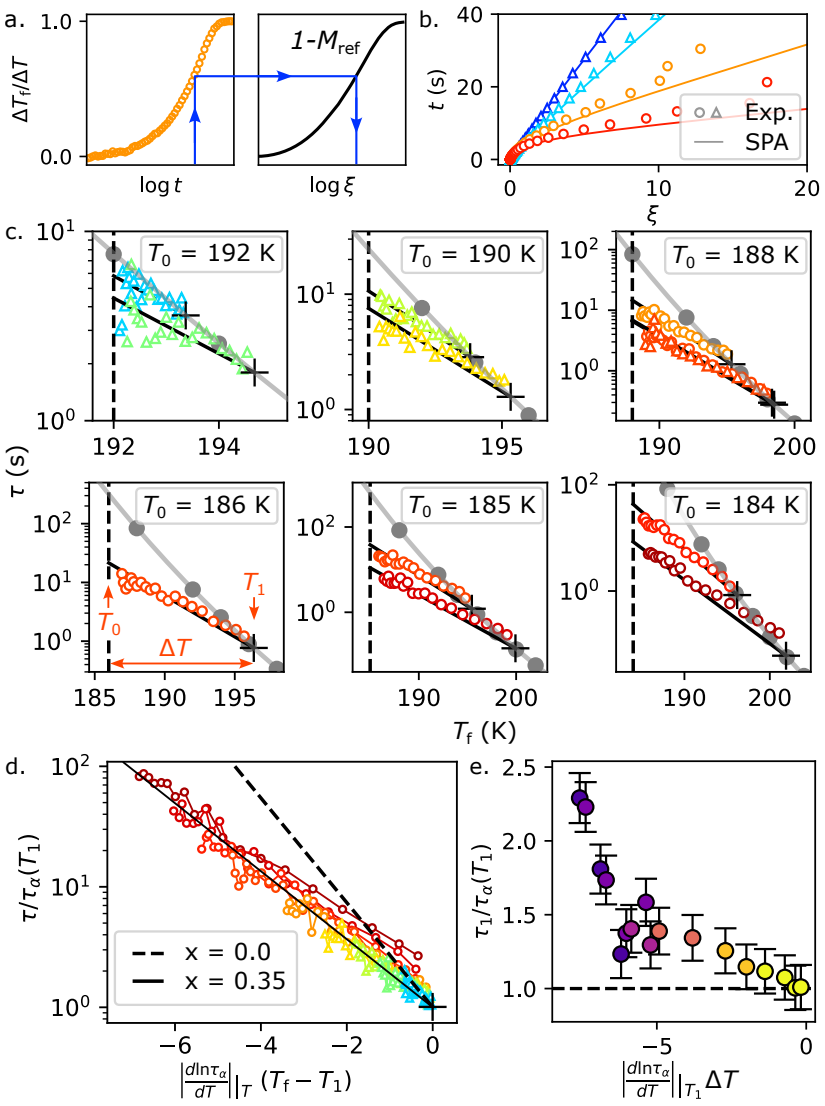

FIG. 3. (a) Schematic showing the determination of $\xi(t)$ by combining an experimental dataset (left) and the reference memory kernel (right). (b) Observer time t as a function of the material time ξ for some of the data shown in fig. 2a with the same colorcode. (c) Out of equilibrium relaxation time $\tau(T_1, T_f)$, computed assuming the validity of the TN, as a function of T_f (colored markers). The grey markers and solid lines correspond to τ_α. The vertical dashed lines locate the initial fictive temperature T_0 while black crosses locate the final equilibrium state at T_1. The solid black lines correspond to the SPA with $x = 0.35$. (d) Out-of-equilibrium relaxation time as a function of the distance from equilibirum plotted in a way that would lead for the SPA to a collapse on a straight line. The black solid line corresponds to $x = 0.35$. (e) The ratio of the final relaxation time τ_1 deduced in the TN framework with the final equilibrium relaxation time as a function of the step amplitude from $T_0 = 184$ K (dark purple) to 193 K (yellow).

ultrastable glasses, also called rejuvenation, was shown, both experimentally and numerically, to be very heterogeneous [33–35, 48] with patches of equilibrated liquid nucleating and growing inside a matrix of still far-from-equilibrium material. By varying the initial stability of the glass, Vila-Costa *et al.* [35] have evidenced a transition between this heterogeneous mechanism and a progressive and cooperative behavior more in line with what we observe in the present work. This was rationalized by the strong dynamic contrast that can exist between the out-of-equilibrium initial state and the final equilibrated liquid. It could be quantified by a threshold separating the two regimes at a transformation time $(180 \pm 60\tau_\alpha(T_1))$ for a TBD glass. In the present work on glycerol we are significantly below this limit with a transformation time reaching at maximum $40\tau_\alpha(T_1)$ for $\Delta T = 17.9$ K. But there likely is a smooth transition connecting the SPA/TN compatible homogeneous mechanism to the heterogeneous picture. In this region, it should become harder and harder to characterize the state of the system with only one quantity (for example T_f) and it is something we observe for the largest step amplitudes tested

in this work with an increasing difference in T_f obtained from C' and C'' (see SI). For larger steps, more useful physical information could be obtained by measuring, during aging, the dielectric loss much closer to the α relaxation frequency as it is done for example in high electric field aging experiments [40]. This should be made possible by the large transformation time allowing to use a probe frequency close to the final relaxation rate.

We further improved the experimental method described in ref. [21] that now allows to set a supercooled liquid out-of-equilibrium by applying upward temperature steps with a wide range of amplitude while measuring its dielectric response during reequilibration. The significant separation between the heating time and the relaxation time of the system, allowed us to perform ideal temperature step experiments for relative amplitude reaching 10 %. For a fragile liquid such as glycerol, this corresponds to a contrast between initial and final relaxation time reaching 2×10^4, thus leading to significant non-linearity in the response. The same setup was used to perform experiments for small temperature steps close to the linear regime. We constructed a fictive temperature consistent with both real and imaginary parts of the dielectric measurements for almost the whole range of amplitude steps. The material time approach in its simplest form (the SPA) was shown to give an excellent agreement for steps reaching a few percent of relative amplitude, in agreement with the literature. In the TN framework, and relying on the response measured at small amplitudes, we deduced the out-of-equilibrium relaxation time. We showed that the concept of material time, based on the idea of a memory-less relaxation time, progressively shows its limits as $\Delta T/T_1$ exceeds a few percent. Notably, it appeared that the TN could not be extended beyond the SPA by assuming a more complex form for the relaxation time or by pushing further its Taylor expansion. In other words, for the molecular glass former studied here, the TN approach and its simpler form, the SPA, fail simultaneously. In the future, it would be interesting to test this on other glassformers. The experimental setup presented in this work could be pushed further in order to reach a wider range of temperature step amplitude with the hope of probing aging following upward steps continuously from the quasi-linear regime to the heterogeneous one.

I. MATERIALS AND METHODS

Materials and methods for this study can be found in the Supporting Information.

Experimental methods. Determination of the α relaxation time, of the equilibrium relaxation kernel, of the fictive temperature from dielectric measurements. Justification of the step ideality. Application of the SPA and determination of the non-linearity parameter related to density scaling concepts.

The authors are grateful to LABEX PALM, IRAMIS Institute and Paris-Saclay University for financial support. This work was supported by ANR PIA funding: ANR-20-IDEES-0002.

[1] C. A. Angell, K. L. Ngai, G. B. McKenna, P. F. McMillan, and S. W. Martin, Relaxation in glassforming liquids and amorphous solids, J. Appl. Phys. **88**, 3113 (2000).
[2] O. Narayanaswamy, A model of structural relaxation in glass, J. Am. Ceram. Soc. **54**, 491 (1971).
[3] J. Y. Raty, W. Zhang, J. Luckas, C. Chen, R. Mazzarello, C. Bichara, and M. Wuttig, Aging mechanisms in amorphous phase-change materials, Nat. Commun. **6**, 7467 (2015).
[4] Y. Huang and D. Paul, Physical aging of thin glassy polymer films monitored by gas permeability, Polymer **45**, 8377 (2004).
[5] S. Vyazovkin and I. Dranca, Effect of physical aging on nucleation of amorphous indomethacin, J. Phys. Chem. B. **111**, 7283 (2007).
[6] L. Berthier and G. Biroli, Theoretical perspective on the glass transition and amorphous materials, Rev. Mod. Phys. **83**, 587 (2011).
[7] F. Arceri, F. P. Landes, L. Berthier, and G. Biroli, A statistical mechanics perspective, on glasses and aging, in *Encyclopedia of Complexity and Systems Science*, edited by R. A. Meyers (Springer Berlin Heidelberg, Berlin, Heidelberg, 2020) pp. 1–68.
[8] L. Grassia and A. D'Amore, Constitutive law describing the phenomenology of subyield mechanically stimulated glasses, Phys. Rev. E **74**, 021504 (2006).
[9] J. P. Gabriel and R. Richert, Comparing two sources of physical aging: Temperature vs electric field, J. Chem. Phys. **159**, 164502 (2023).
[10] H. R. Lillie, Viscosity-time-temperature relations in glass at annealing temperatures, J. Am. Ceram. Soc. **16**, 619 (1933).
[11] A. J. Kovacs, Transition vitreuse dans les polymères amorphes. etude phénoménologique, in *Fortschritte der hochpolymeren-forschung* (Springer, Berlin, Heidelberg, 1964) pp. 394–507.
[12] R. L. Leheny and S. R. Nagel, Frequency-domain study of physical aging in a simple liquid, Phys. Rev. B **57**, 5154 (1998).
[13] P. Lunkenheimer, R. Wehn, U. Schneider, and A. Loidl, Glassy Aging Dynamics, Phys. Rev. Lett. **95**, 055702 (2005).
[14] T. Hecksher, N. B. Olsen, K. Niss, and J. C. Dyre, Physical aging of molecular glasses studied by a device allowing for rapid thermal equilibration, J. Chem. Phys. **133**, 174514 (2010).
[15] B. Riechers, L. A. Roed, S. Mehri, T. S. Ingebrigtsen, T. Hecksher, J. C. Dyre, and K. Niss, Predicting nonlinear physical aging of glasses from equilibrium relaxation via the material time, Sci. Adv. **8**, eabl9809 (2022).

[16] V. Di Lisio, V.-M. Stavropoulou, and D. Cangialosi, Physical aging in molecular glasses beyond the α relaxation, J. Chem. Phys. **159**, 064505 (2023).

[17] K. Moch, R. Böhmer, and C. Gainaru, Temperature oscillations provide access to high-order physical aging harmonics of a glass forming melt, J. Chem. Phys. **159**, 221102 (2023).

[18] R. F. Lancelotti, E. D. Zanotto, and S. Sen, Kinetics of physical aging of a silicate glass following temperature up-and down-jumps, J. Chem. Phys. **160**, 034504 (2024).

[19] G. W. Scherer, Volume relaxation far from equilibrium, J. Am. Ceram. Soc. **69**, 374 (1986).

[20] K. Niss, Mapping isobaric aging onto the equilibrium phase diagram, Phys. Rev. Lett. **119**, 115703 (2017).

[21] M. Hénot and F. Ladieu, Non-linear physical aging of supercooled glycerol induced by large upward ideal temperature steps monitored through cooling experiments, J. Chem. Phys. **158**, 224504 (2023).

[22] A. Q. Tool, Relation between inelastic deformability and thermal expansion of glass in its annealing range, J. Am. Ceram. Soc. **29**, 240 (1946).

[23] I. M. Hodge, Physical aging in polymer glasses, Science **267**, 1945 (1995).

[24] T. Hecksher, N. B. Olsen, and J. C. Dyre, Communication: Direct tests of single-parameter aging, J. Chem. Phys. **142**, 241103 (2015).

[25] L. A. Roed, T. Hecksher, J. C. Dyre, and K. Niss, Generalized single-parameter aging tests and their application to glycerol, J. Chem. Phys. **150**, 044501 (2019).

[26] J. Málek, Structural relaxation rate and aging in amorphous solids, J. Phys. Chem. C **127**, 6080 (2023).

[27] I. M. Douglass and J. C. Dyre, Distance-as-time in physical aging, Phys. Rev. E **106**, 054615 (2022).

[28] R. Peredo-Ortiz, M. Medina-Noyola, T. Voigtmann, and L. F. Elizondo-Aguilera, "inner clocks" of glass-forming liquids, J. Chem. Phys. **156**, 244506 (2022).

[29] T. Böhmer, J. P. Gabriel, L. Costigliola, J.-N. Kociok, T. Hecksher, J. C. Dyre, and T. Blochowicz, Time reversibility during the ageing of materials, Nat. Phys. , 1 (2024).

[30] R. Kaur, D. Bhattacharya, U. S. Cubeta, and V. Sadtchenko, Glass softening in the limit of high heating rates: Heterogeneous devitrification kinetics on nano, meso, and micrometer scale, J. Chem. Phys. **158**, 164507 (2023).

[31] S. F. Swallen, K. L. Kearns, M. K. Mapes, Y. S. Kim, R. J. McMahon, M. D. Ediger, T. Wu, L. Yu, and S. Satija, Organic glasses with exceptional thermodynamic and kinetic stability, Science **315**, 353 (2007).

[32] S. Singh, M. D. Ediger, and J. J. De Pablo, Ultrastable glasses from in silico vapour deposition, Nat. Mater. **12**, 139 (2013).

[33] M. Ruiz-Ruiz, A. Vila-Costa, T. Bar, C. Rodríguez-Tinoco, M. Gonzalez-Silveira, J. A. Plaza, J. Alcalá, J. Fraxedas, and J. Rodriguez-Viejo, Real-time microscopy of the relaxation of a glass, Nat. Phys. , 1 (2023).

[34] C. Herrero, C. Scalliet, M. Ediger, and L. Berthier, Two-step devitrification of ultrastable glasses, Proc. Natl. Acad. Sci. **120**, e2220824120 (2023).

[35] A. Vila-Costa, M. Gonzalez-Silveira, C. Rodríguez-Tinoco, M. Rodríguez-López, and J. Rodriguez-Viejo, Emergence of equilibrated liquid regions within the glass, Nat. Phys. **19**, 114 (2023).

[36] Z. Chen, A. Sepúlveda, M. Ediger, and R. Richert, Dielectric spectroscopy of thin films by dual-channel impedance measurements on differential interdigitated electrode arrays, Eur. Phys. J. B **85**, 1 (2012).

[37] E. Dzik, P. Datin, J.-P. Dognon, C. Fajolles, C. Wiertel-Gasquet, D. Carrière, and F. Ladieu, Simultaneously measuring the dichroism and the dielectric response of an azobenzene-doped organic glass former, Rev. Sci. Instrum. **94**, 123904 (2023).

[38] T. Hecksher, N. B. Olsen, and J. C. Dyre, Fast contribution to the activation energy of a glass-forming liquid, Proc. Natl. Acad. Sci. **116**, 16736 (2019).

[39] J. C. Mauro, R. J. Loucks, and P. K. Gupta, Fictive temperature and the glassy state, J. Am. Ceram. Soc. **92**, 75 (2009).

[40] B. Riechers and R. Richert, Rate exchange rather than relaxation controls structural recovery, Phys. Chem. Chem. Phys. **21**, 32 (2019).

[41] C. Moynihan, P. Macedo, C. Montrose, C. Montrose, P. Gupta, M. DeBolt, J. Dill, B. Dom, P. Drake, A. Easteal, *et al.*, Structural relaxation in vitreous materials, Ann. N. Y. Acad. Sci. **279**, 15 (1976).

[42] R. Richert, J. P. Gabriel, and E. Thoms, Structural relaxation and recovery: A dielectric approach, J. Phys. Chem. Lett. **12**, 8465 (2021).

[43] K. Niss, A density scaling conjecture for aging glasses, J. Chem. Phys. **157**, 054503 (2022).

[44] C. Alba-Simionesco, D. Kivelson, and G. Tarjus, Temperature, density, and pressure dependence of relaxation times in supercooled liquids, J. Chem. Phys. **116**, 5033 (2002).

[45] K. Z. Win and N. Menon, Glass transition of glycerol in the volume-temperature plane, Phys. Rev. E **73**, 040501 (2006).

[46] I. V. Blazhnov, N. P. Malomuzh, and S. V. Lishchuk, Temperature dependence of density, thermal expansion coefficient and shear viscosity of supercooled glycerol as a reflection of its structure, J. Chem. Phys. **121**, 6435 (2004).

[47] J. C. Mauro, D. C. Allan, and M. Potuzak, Nonequilibrium viscosity of glass, Phys. Rev. B **80**, 094204 (2009).

[48] A. Vila-Costa, J. Ràfols-Ribé, M. González-Silveira, A. Lopeandia, L. Abad-Muñoz, and J. Rodríguez-Viejo, Nucleation and growth of the supercooled liquid phase control glass transition in bulk ultrastable glasses, Phys. Rev. Lett. **124**, 076002 (2020).

Supporting Information : Crossing the Frontier of Validity of the Material Time Approach in the Aging of a Molecular Glass

Marceau Hénot,[1,*] Xuan An Nguyen,[1] and François Ladieu[1]

[1] *SPEC, CEA, CNRS, Université Paris-Saclay, CEA Saclay Bat 772, 91191 Gif-sur-Yvette Cedex, France.*

CONTENTS

I. EXPERIMENTAL METHODS

The experimental setup, shown in fig. 1a of the main text, consists in a 25 μm thick layer of glycerol (purchased from Sigma-Aldrich, $\geq$ 99.5 %), sandwiched between a heating plate and a set of Interdigitated Electrodes (IDE) separated by a mylar spacer. The former is a 1 mm thick glass plate covered by a 80 nm thick ITO (Indium-Tin-Oxyde) layer whose electrical resistance between each side is $r = 49\ \Omega$ (copper layers are vapor-deposited on the sides to ensure electrical contact). The heating power is supplied by a Fontaine ALS3020 DC power supply and the pulse sequence is controlled by a MOSFET transistor and an Arduino Due micro-controller.

The IDE consists of 240 pairs of 3 mm long, 100 nm thick copper lines of width $w = 6$ µm and separated by each other by a distance $l = w$. They were made on a 1 mm thick glass plate using optical lithography and a lift-off process (with S1805 and LOL2000 photoresists). The IDE capacitance $C = C' - jC''$ was measured by associating it with a $R = 50$ kΩ resistor, by applying (with a SR830) a sinusoidal voltage $v_{\rm alim}(t)$ of RMS amplitude $\langle v_{\rm alim}^2 \rangle = 4$ V and frequency $f = 1.12$ or 3 kHz to the whole. Both $v_{\rm alim}(t)$ and the voltage across the resistor $v_{\rm R}(t)$ were acquired using a RTB2004 oscilloscope. The amplitude ratio and phase shift between both signals were determined for each period, allowing to obtain $C'(t)$ and $C''(t)$ (see fig. 1c of the main text). The measurements performed at $f = 1.12$ kHz (for the smaller ΔT) were averaged between 220 and 25 times depending on the noise level. For larger ΔT, at $f = 3.0$ kHz only one measurement was made.

The heating pulse sequence required to maintain the temperature constant is determined using a 1D thermal numerical simulation is used for $t < 0.5$ s [3]. For $t \in [0.5, 50]$ s, it is determined by trial and error using the IDE as a thermometer at $T_0 = 207$ K.

* Corresponding author: marceau.henot@cea.fr

II. DETERMINATION OF $\tau_\alpha(T)$

The complex capacitance $C^\star$ of the IDE is given by:

$$C^\star = \epsilon_0 l_{\text{eq}}(\epsilon^\star + \epsilon_{\text{subtrate}}) \tag{S1}$$

where ϵ_0 is the dielectric permittivity of vacuum, $\epsilon^\star$ and $\epsilon_{\text{substrate}}$ are the complex relative permittivity of the liquid and of the substrate respectively and $l_{\text{eq}} = Nl$ with N the number lines attached to each electrode and l their length.

The dissipation in the substrate can be neglected, and the imaginary part of the IDE capacitance is directly proportional to the dielectric loss of the liquid $C'' \propto \epsilon''$.

The spectra $C''(w)$ shown in fig. S1a were measured at equilibrium at different temperatures. The α peak is well visible for $T \geq 194$ K and the α relaxation time (solid markers in fig. S1c) was obtained from the peak angular frequency $\tau_\alpha = 1/\omega_\alpha$. For $T \leq 190$ K for which the peak was not visible, τ_α was determined by taking advantage of the fact that the maximum of the dielectric loss is proportional to $1/T$ up to negligible corrections and thus that all spectra should collapse (at least close to the α peak) when plotted as TC'' as function of $\omega\tau_\alpha$ (see fig. S1b). The values of τ_α obtained this way are shown in fig. S1c with empty markers.

A VFT law $\tau_\alpha(T) = \tau_0 \exp(\frac{A}{T-T_{\text{K}}})$ was fitted on the data and is shown in black in fig. S1c, with best parameters $\tau_0 = 0.96$ fs, $A = 2380$ K and $T_{\text{K}} = 127$ K.

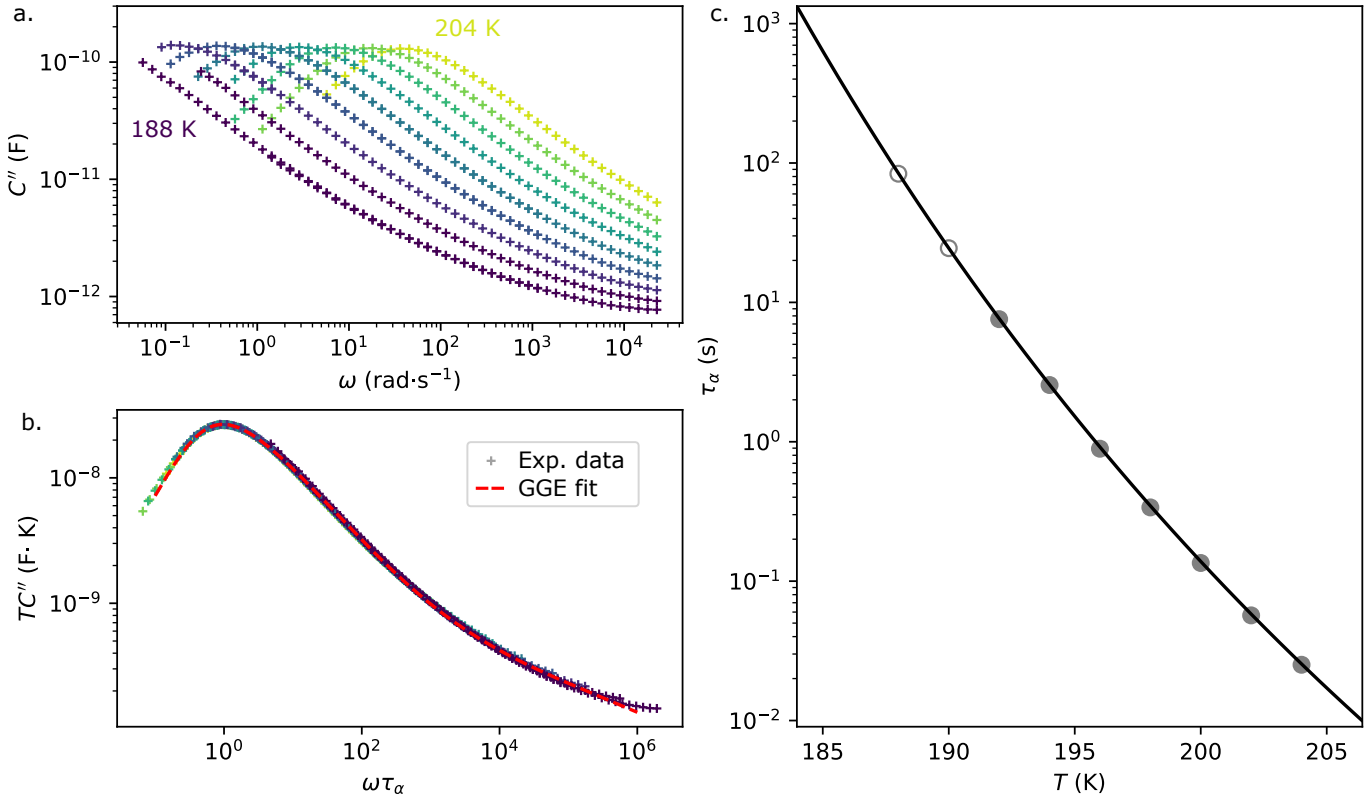

FIG. S1. (a) Imaginary part C'' of the capacitance formed by the comb-type electrode as a function of the pulsation ω measured at equilibrium at temperature ranging from 188 to 204 K with 2 K increment. (b) Same data vertically scaled by T and horizontally scaled by τ_α. The red dashed line is a GGE fit [4]. (c) Corresponding values of τ_α as function of T. Solid markers correspond to a determination from the α peak in a. while empty markers are obtained from the collapse of the high frequency wing in b. The solid line is a VFT fit.

III. EQUILIBRIUM RELAXATION KERNEL M_α

The equilibrium relaxation kernel corresponds to the Laplace-Fourier transform of the dielectric spectra $\epsilon^\star(\omega)$ [5]. However because this method is sensitive to noise, we instead relied on the relaxation time distribution $G(\ln\tau)$.

The dynamics of glycerol can be described by the GGE distribution introduced by Blochowicz *et al.* [4] with the following expression: GGE fit [4].

$$G_{\mathrm{GGE}}(\ln\tau) = N_{\mathrm{GGE}} e^{(-\beta/\alpha)(\tau/\tau_0)^\alpha} \left(\frac{\tau}{\tau_0}\right)^\beta \left(1 + \left(\frac{\tau\sigma}{\tau_0}\right)^{\gamma-\beta}\right) \tag{S2}$$

Where N_{GGE} is a normalization coefficient, τ_0 is a time scale, α, β parameterize the α peak and γ, σ parameterize the excess wing. The loss spectra is obtain from the imaginary part of:

$$\frac{\epsilon(\omega) - \epsilon_\infty}{\Delta\epsilon} = \int_{-\infty}^{\infty} G(\ln\tau) \frac{1}{1 + j\omega\tau} d\ln\tau \tag{S3}$$

The following parameters are used in fig. S1b: $\alpha = 10$, $\beta = 0.8$, $\gamma = 0.2$ and $\sigma = 300$ and lead to a very good agreement. They are close to what is reported in ref [4] for the same system. Here the time is made dimensionless using τ_α and the time scale $\log\tau_0 = 0.28$ is chosen so that the α peak occurs at 1.

The α memory kernel is then obtained from:

$$M_\alpha(\xi) = \int_{-\infty}^{\infty} G(\ln\tau) e^{-\xi/\tau} d\ln\tau \tag{S4}$$

The result is shown with a dashed blue line in fig. 2b of the main text.

IV. FICTIVE TEMPERATURE FROM DIELECTRIC MEASUREMENTS

The fictive temperature was obtained from dielectric measurements in two steps:

- The measured values of $C'(t)$ and $C''(t)$ were first converted in temperature units $T_{\mathrm{from\ C}}(t)$ by using a mapping measured at equilibrium (shown in fig. S2). The result is shown for example in fig. 1d of the main text and in fig. S4 (top).
- The glassy response of the system, well visible during the heating phase, was then subtracted. The fictive temperature was obtained from : $\Delta T_{\mathrm{from\ }C}(t) = \kappa\Delta T + (1-\kappa)\Delta T_{\mathrm{f}}(t)$ where κ was determined to ensure that $\Delta T_{\mathrm{f}}(t=0) = 0$. The values of κ are shown in fig. S3.

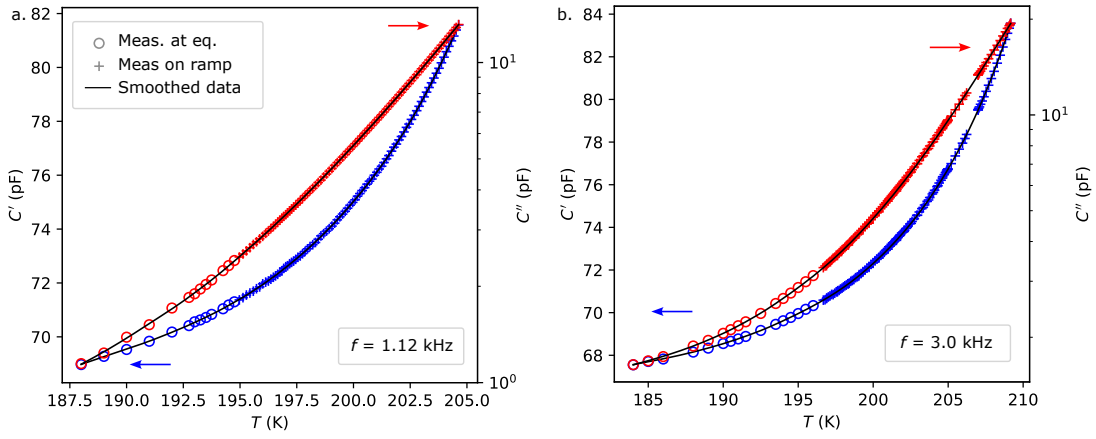

FIG. S2. Real (blue) and imaginary parts (red) of the capacitance measured at equilibrium at $f = 1120$ Hz (a) and 3000 Hz (b) as a function of T and used in this work to obtain $T_{\mathrm{from\ }C}$. Circles correspond to measurement at equilibrium while crosses correspond to measurement during positive and negative temperature ramps with rate < 0.4 K/min. The black lines correspond to a cubic interpolation of the smoothed data.

While at small step amplitude, the real and imaginary parts of the capacitance gave the exact same result when converted into temperature units and thus led to the same fictive temperature, it is not the case for very large temperature steps. This is visible in fig. S3 and S4 with C' and C'' showing different sensitivity to the glassy response leading to different values of κ. For $\Delta T = 17.9$ K, this makes a visible difference in the obtained fictive temperature (see fig. S4 bottom right).

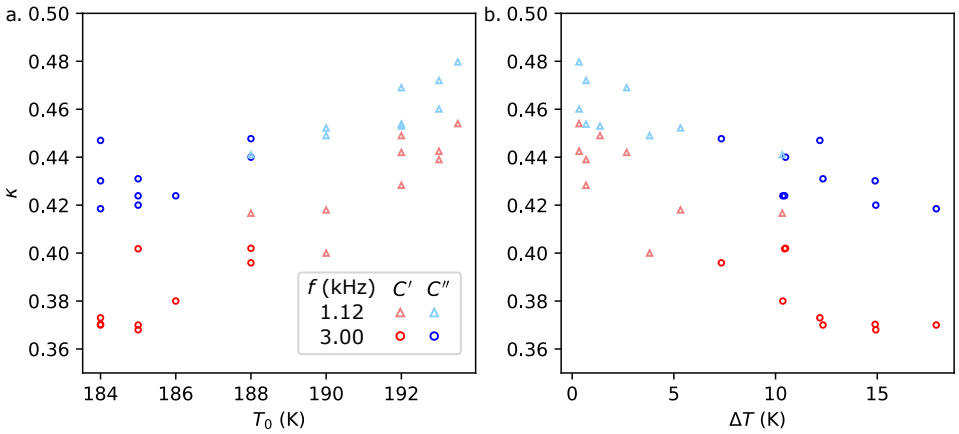

FIG. S3. Fraction of the fast response κ plotted as a function of the initial temperature T_0 (a) and of the step amplitude ΔT (b). In this work the parameters T_0 and ΔT are correlated (with T_0 decreasing for ΔT increasing).

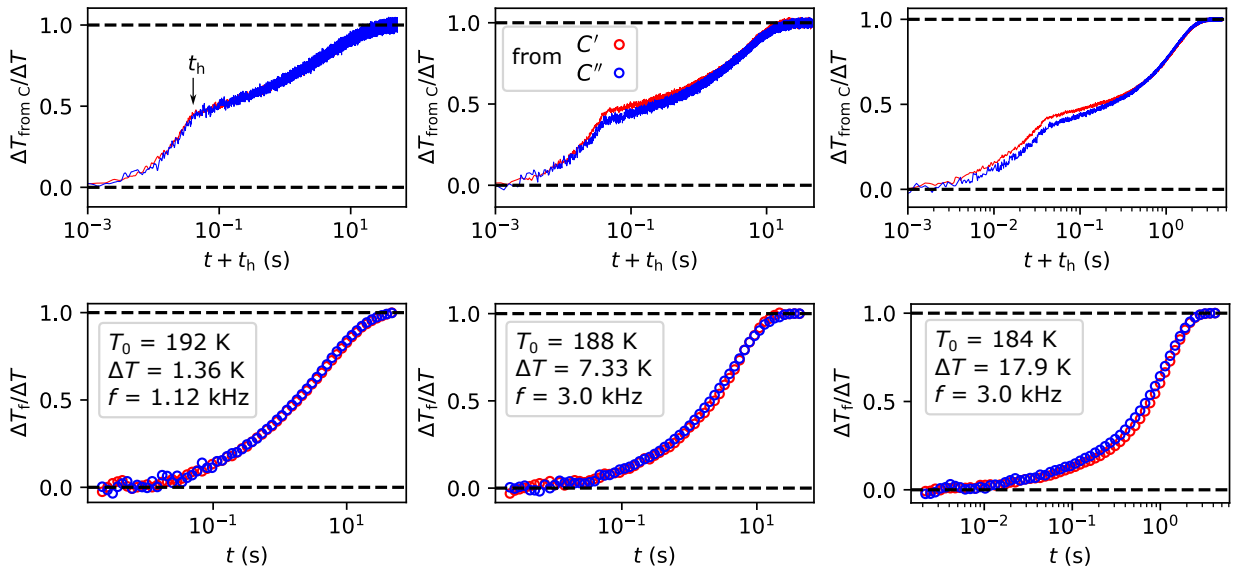

FIG. S4. Normalized temperature obtained by mapping the capacitance $C'(t)$ (red) and $C''(t)$ (blue) with the equilibrium values (top) and normalized fictive temperature (bottom) for three temperature steps of increasing amplitude (left to right).

V. APPLICATION OF THE SPA MODEL

V.1. Determination of the memory kernel

The reference memory kernel $M_{\mathrm{ref}}(\xi)$ was obtained here from the experiments corresponding to the smallest amplitudes ($\Delta = 0.34$ and 0.68 K). Although these amplitudes are too large to be in the linear response regime, the memory kernel that can be obtained by using the SPA is only weakly dependent on the exact value of x in the range $[0.1; 0.6]$ as shown in fig. S5.

Fig. S6 illustrates the application of the SPA to the data shown in fig. 2 of the main text with different values of x from 0.2 to 0.4. It is visible that no value of x can lead to a good agreement for the largest step amplitude. The agreement between the experimental data and the SPA can be quantified by computing the mean of the squared difference between the data and the model (without considering the data corresponding to $\xi < 10^{-3}$ which are very noisy). The result is shown in fig. S7. It is visible that $x = 0.35$ leads to the best agreement and that this agreement becomes worse when ΔT is increased.

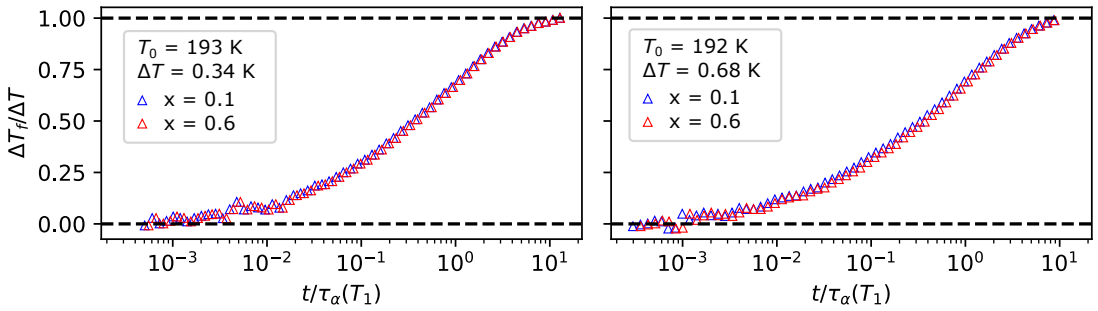

FIG. S5. Illustration of the low sensitivity of ξ_{SPA} to x for small temperature steps. Normalized liquid response as a function of ξ computed using the SPA with $x = 0.1$ (blue) and $x = 0.6$ (red).

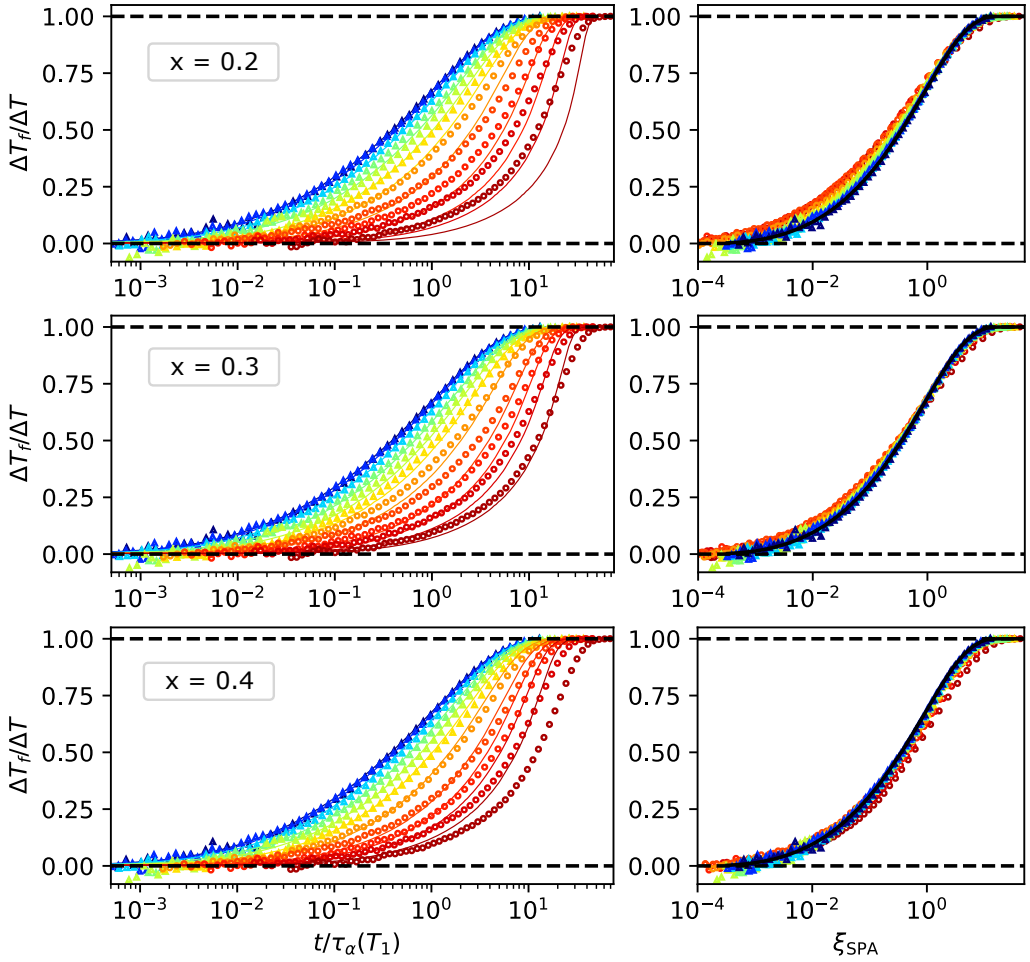

FIG. S6. Same quantities than fig. 2 of the main text. (Left) The experimental data (markers) are compared with the SPA model (solid lines) for different values of x. (Right) Normalized response as a function of the material time computed using the SPA model.

V.2. Step ideality

In this work, the temperature steps were assumed ideal. For the moderate temperature steps, this can be checked *a posteriori* with the help of the SPA. A quantitative characterization of the ideality is the ratio $\tau(0^+)/t_{\mathrm{h}}$ with $\tau(0^+) = \tau(T = T_1, T_{\mathrm{f}} = T_0)$ that should be as large as possible. Due to the nature of the present experiments, the total duration $t_{\max}$ is limited. A trade-off has thus to be made between this ratio and $t_{\max}$ that should be at least 100 times larger than the final relaxation time $\tau_\alpha(T_1)$ in order to reach equilibrium. The most constraining case

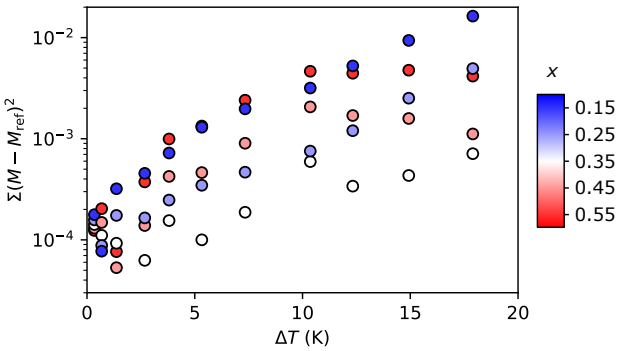

FIG. S7. Comparison between experimental data and the SPA prediction for the memory kernel for different values of x. The sum of the squared difference between the memory kernel obtained from the data and the reference kernel is shown as a function of the temperature step amplitude.

corresponds to the smallest step amplitude for which $\tau(0^+) \approx \tau_\alpha(T_1)$. In this case T_0 is chosen so that t_h, $\tau_\alpha(T_1)$ and $t_{\max}$ are evenly log spaced. Increasing the step amplitude is favorable in that regard as $\tau(0^+)$ can become much larger than $\tau_\alpha(T_1)$. In all cases, T_0 was chosen to ensure that $t_\mathrm{h}/\tau(0^+) \in [100 - 250]$. All this relies on the fact that the SPA applies, which is less and less the case as ΔT increases.

For larger steps, we checked that the initial evolution rate of the normalized fictive temperature with respect to the heating time was not higher for the largest steps than for the smallest ones. Fig. S8 shows the normalized fictive temperature evolution for the data shown in fig. 2a of the main text. The initial temperature T_0 is decreased when ΔT is increased in order to prevent as much as possible relaxation during the heating phase. For all experiments, this leads to the same initial evolution of the normalized fictive temperature. In particular, it is the same for the largest and the smallest temperature step amplitudes.

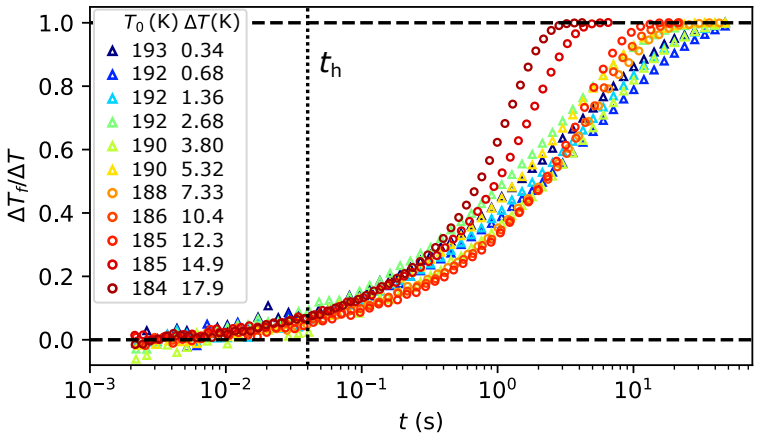

FIG. S8. Normalized fictive temperature evolution as a function of time (with $t = 0$ corresponding to the end of the heating phase). The heating time is shown as a vertical dashed line.

VI. DETERMINATION OF THE NON-LINEARITY PARAMETER USING DENSITY SCALING CONCEPTS

VI.1. Density scaling at equilibrium

The density scaling approach consists in accounting for the temperature T and the specific volume v dependence of the equilibrium relaxation time through one parameter Γ [6, 7]:

$$\tau_\alpha(T, v) = f(\Gamma), \qquad \Gamma = \frac{1}{Tv^\gamma} \tag{S5}$$

where γ is the density scaling exponent which is system dependent and f is a function that can be fitted on the experimental data (it can be for instance a VFT or an Arrhenius law).

VI.2. Approach of Di Lisio *et al.* [1]

The approach of Di Lisio *et al.* [1] is to estimate the out-of-equilibrium relaxation time $\tau(T, T_\mathrm{f})$ using the density scaling approach with the phonon bath temperature T and the out-of-equilibrium specific volume v.

Let us consider an ideal temperature step from T_0 to $T_1 = T_0 + \Delta T$ and denote v_0 and v_1 the equilibrium initial and final specific volume. The change in v is related to the liquid expansion coefficient α_l by: $v_1 - v_0 = \alpha_\mathrm{l}\Delta T$. Just after the temperature step, the out-of-equilibrium specific volume $v(0^+)$ takes an intermediate value: $v_1 - v(0^+) = \Delta\alpha\Delta T$ with $\Delta\alpha = \alpha_\mathrm{l} - \alpha_\mathrm{g}$ where α_g is the glassy expansion coefficient. The relaxation time $\tau(0^+) = \tau(T = T_1, T_\mathrm{f} = T_0)$ is thus:

$$\tau(0^+) = f\left(\frac{1}{T_1 v(0^+)^\gamma}\right) = f\left(\frac{1}{T_1(v_1 - \Delta\alpha\Delta T)^\gamma}\right) \tag{S6}$$

In the following we consider the small ΔT limit (compared to $v_1/\Delta\alpha$) in order to quantitatively compare this approach to the SPA model. A first order Taylor expansion of $\ln\tau_0^+$ gives:

$$\ln\tau(0^+) = \ln f\left(\frac{1}{T_1 v_1^\gamma(1 - \frac{\Delta\alpha\Delta T}{v_1})^\gamma}\right) \approx \ln f\left(\Gamma_1\left(1 + \gamma\frac{\Delta\alpha\Delta T}{v_1}\right)\right) \approx \ln f\left(\Gamma_1\right) + \Gamma_1\gamma\frac{\Delta\alpha\Delta T}{v_1}\frac{d\ln f}{d\Gamma}|_{\Gamma_1} \tag{S7}$$

On the other side, if we assume that $\ln\tau(T, T_\mathrm{f}) = x\ln\tau_\alpha(T) + (1-x)\ln\tau_\alpha(T_\mathrm{f})$ with $\tau_\alpha(T)$. A similar first order Taylor expansion gives:

$$\ln\tau_0^+ = x\ln\tau_\alpha(T_1) + (1-x)\ln\tau_\alpha(T_1 - \Delta T) \approx x\ln\tau_\alpha(T_1) + (1-x)(\ln\tau_\alpha(T_1) - \Delta T\frac{d\ln\tau_\alpha}{dT}|_{T_1} \tag{S8}$$

$$\approx \ln\tau_\alpha(T_1) - (1-x)\Delta T\frac{d\ln\tau_\alpha}{dT}|_{T_1} \tag{S9}$$

An identification between eq. S7 and eq. S9 leads to:

$$(1-x) = -\gamma\Gamma_1\frac{\Delta\alpha}{v_1}\frac{\frac{d\ln f}{d\Gamma}|_{\Gamma_1}}{\frac{d\ln\tau_\alpha}{dT}|_{T_1}} \tag{S10}$$

This formula can be applied to the specific case of glycerol in order to determine a value of x. Win and Menon [7] measured $\tau_\alpha(\Gamma)$ for glycerol and reported $\gamma = 1.4$. An Arrhenius fit of their data ($\tau_\alpha(\Gamma) \propto e^{-C\Gamma}$) gives $C = (1.1 \pm 0.1)\cdot 10^4$ K$(\mathrm{g/cm^3})^\gamma$ around $T = 200$ K and ambient pressure. Using a VFT fit for $\tau_\alpha(T)$ (with $A = 2380$ K and $T_\mathrm{K} = 127$ K), eq. S10 becomes:

$$(1-x) = \gamma\Gamma_1\frac{\Delta\alpha}{v_1}\frac{C(T_1 - T_\mathrm{K})^2}{A} \tag{S11}$$

With $\Delta\alpha = 4.10^{-4}$ K^{-1} [8] and $v(200\text{ K}) = 0.76$ cm$^3\cdot$g^{-1}, this leads to $x \approx 0.86 \pm 0.02$.

VI.3. Niss conjecture [2]

The density scaling approach can be formulated in such a way as to reveal an activation energy [6] which depends on T and v.

$$\tau_\alpha(T, v) = \tau_0\exp(\Gamma F(\Gamma)), \qquad \Gamma = \frac{e(v)}{T} \tag{S12}$$

where τ_0 is a microscopic time. This is equivalent to eq. S5 but gives a physical interpretation of the role of Γ: the first term in factor $\Gamma = \frac{e(v)}{T}$ contains an energy scale e of the barriers height in the energy landscape (that depends only on v) and the thermal energy of the phonon bath set by T. The topology of the energy landscape is characterized by the function F that depends on both v and T through Γ.

In this framework, Niss [2] makes the conjecture that out-of-equilibrium, the energy scale is set by the volume v and the kinetic bath temperature T (the first term in factor is thus $\Gamma = e(v)/T$) while the topology of the energy landscape is set by a fictive Γ_f that has the constrain of being continuous following a temperature jump:

$$\tau = \tau_0 \exp(\Gamma F(\Gamma_\mathrm{f})) \tag{S13}$$

This means that, just after a temperature step:

$$\tau(0^+) = \tau_0 \exp\left(\frac{e(v(0^+))}{T_1} F\left(\frac{e(v_0)}{T_0}\right)\right) \tag{S14}$$

This result is different from eq. S6. As $\Gamma_0 > \Gamma(0^+)$ and $F(\Gamma)$ is an increasing function [6], the following inequality can be written:

$$\tau_0 \exp\left(\Gamma(0^+) F\left(\Gamma_0\right)\right) > \tau_0 \exp\left(\Gamma(0^+) F\left(\Gamma(0^+)\right)\right) \tag{S15}$$

$$\tau_\mathrm{Niss}(0^+) > \tau_{\text{Di Lisio et al.}}(0^+) \tag{S16}$$

Niss conjecture thus lead to value of x smaller than 0.85.

---

[1] Di Lisio, V.; Stavropoulou, V.-M.; Cangialosi, D. Physical aging in molecular glasses beyond the α relaxation. *J. Chem. Phys.* **2023**, *159*, 064505.

[2] Niss, K. A density scaling conjecture for aging glasses. *J. Chem. Phys.* **2022**, *157*, 054503.

[3] Hénot, M.; Ladieu, F. Non-linear physical aging of supercooled glycerol induced by large upward ideal temperature steps monitored through cooling experiments. *J. Chem. Phys.* **2023**, *158*, 224504.

[4] Blochowicz, T.; Tschirwitz, C.; Benkhof, S.; Rössler, E. Susceptibility functions for slow relaxation processes in supercooled liquids and the search for universal relaxation patterns. *J. Chem. Phys.* **2003**, *118*, 7544–7555.

[5] Gabriel, J. P.; Richert, R. Comparing two sources of physical aging: Temperature vs electric field. *J. Chem. Phys.* **2023**, *159*, 164502.

[6] Alba-Simionesco, C.; Kivelson, D.; Tarjus, G. Temperature, density, and pressure dependence of relaxation times in supercooled liquids. *J. Chem. Phys.* **2002**, *116*, 5033–5038.

[7] Win, K. Z.; Menon, N. Glass transition of glycerol in the volume-temperature plane. *Phys. Rev. E* **2006**, *73*, 040501.

[8] Blazhnov, I. V.; Malomuzh, N. P.; Lishchuk, S. V. Temperature dependence of density, thermal expansion coefficient and shear viscosity of supercooled glycerol as a reflection of its structure. *J. Chem. Phys.* **2004**, *121*, 6435–6441.